Chimera Ising walls in forced nonlocally coupled oscillators

Yoji Kawamura*
Department of Physics, Graduate School of Sciences, Kyoto University, Kyoto 606-8502, Japan
(Received 12 December 2006; published 9 May 2007)

Nonlocally coupled oscillator systems can exhibit an exotic spatiotemporal structure called a chimera, where the system splits into two groups of oscillators with sharp boundaries, one of which is phase locked and the other phase randomized. Two examples of chimera states are known: the first one appears in a ring of phase oscillators, and the second is associated with two-dimensional rotating spiral waves. In this paper, we report yet another example of the chimera state that is associated with the so-called Ising walls in one-dimensional spatially extended systems. This chimera state is exhibited by a nonlocally coupled complex Ginzburg-Landau equation with external forcing.

DOI: 10.1103/PhysRevE.75.056204 PACS number(s): 05.45.Xt, 82.40.Ck

I. INTRODUCTION

Nonlocally coupled oscillator systems can exhibit a remarkable class of patterns called *chimera*, in which identical oscillators separate sharply into two domains, one coherent and phase locked, the other incoherent and drifting [1–4]. These two groups of oscillators together maintain stable organized patterns in the system. The existence of such patterns was first noticed and explained in a ring of phase oscillators [1], and studied in further detail [3]. Furthermore, it was found that the chimera states also appear in rotating spiral waves in two-dimensional spatially extended systems [2]. Recently, an interesting pattern similar to the chimera states studied in Refs. [1,3] was also found in nonlocally coupled Hodgkin-Huxley equations with excitatory and inhibitory synaptic coupling, where such patterns spontaneously appear as a result of the instability of the uniform state, in contrast to the original chimera that appears when the uniform state is stable [5].

In this paper, we present another simple example of the chimera state associated with the Ising walls in one-dimensional spatially extended systems, which is exhibited by a nonlocally coupled complex Ginzburg-Landau equation (CGLE) with a parametric forcing. Recently, a nonlocally coupled CGLE without forcing has been studied intensively [6–12], and a locally coupled CGLE with forcing has also been investigated widely [13–19]. To our knowledge, Battogtokh considered the nonlocally coupled CGLE with forcing for the first time, and demonstrated various interesting phenomena, e.g., nonequilibrium Ising-Bloch transitions [20]. Here, we will focus only on the chimera Ising wall; it is the simplest one among them, but its theoretical analysis has not yet been carried out.

The organization of the present paper is the following. In Sec. II, we introduce our model and illustrate its normal and chimera Ising walls by numerical simulations. In Sec. III, we reduce our model to the phase model, and numerically demonstrate that the reduced phase model also exhibits the chimera Ising walls. In Sec. IV, a functional self-consistency equation is derived by introducing a space-dependent order parameter, and its numerical solution is compared with the numerical simulation presented in Sec. III. Concluding remarks will be given in the final section.

II. CHIMERA ISING WALLS

We consider the following equation that describes a system of nonlocally coupled limit-cycle oscillators driven by a parametric external forcing:

$$\partial_t A = (1+ic_0)A - (1+ic_2)|A|^2A + K(1+ic_1)(B-A) + \gamma A^*, \tag{1}$$

which we call a forced nonlocally coupled complex Ginzburg-Landau equation. Here c_0, c_1, c_2, K, and γ are real parameters, the complex amplitude $A(x,t)$ represents the state of a local limit-cycle oscillator at location x and time t, and A^* is the complex conjugation of A. The quantity $B(x,t)$ represents the nonlocal coupling defined by

$$B(x,t) = \int dx' G(x-x')A(x',t), \tag{2}$$

$$G(x) = \frac{1}{2}\exp(-|x|), \tag{3}$$

where the nonlocal coupling function $G(x)$ is normalized in the infinite domain. K represents the coupling strength, and c_1 is the phase shift of the coupling [6–12]. The last term γA^* represents the effect of the parametric external forcing with almost double the natural frequency, whose intensity is given by γ, and c_0-c_2 stands for the frequency mismatch [13–19]. In the absence of the coupling and the external forcing, i.e., when $K=\gamma=0$, Eq. (1) is simply given by $\partial_t A=(1+ic_0)A-(1+ic_2)|A|^2A$, which is the simplest limit-cycle oscillator, called the Stuart-Landau oscillator [21,22], so that Eq. (1) describes a system of forced nonlocally coupled oscillators. In addition, Eq. (1) is a normal form that can be derived from a wide class of reaction-diffusion systems near the Hopf bifurcation point under particular assumptions by using the center-manifold reduction method [6,10,13,21].

In our numerical simulations, the continuous medium of size L was discretized using $N=2048$ grid points with suffi-

*Electronic address: kawamura@ton.scphys.kyoto-u.ac.jp

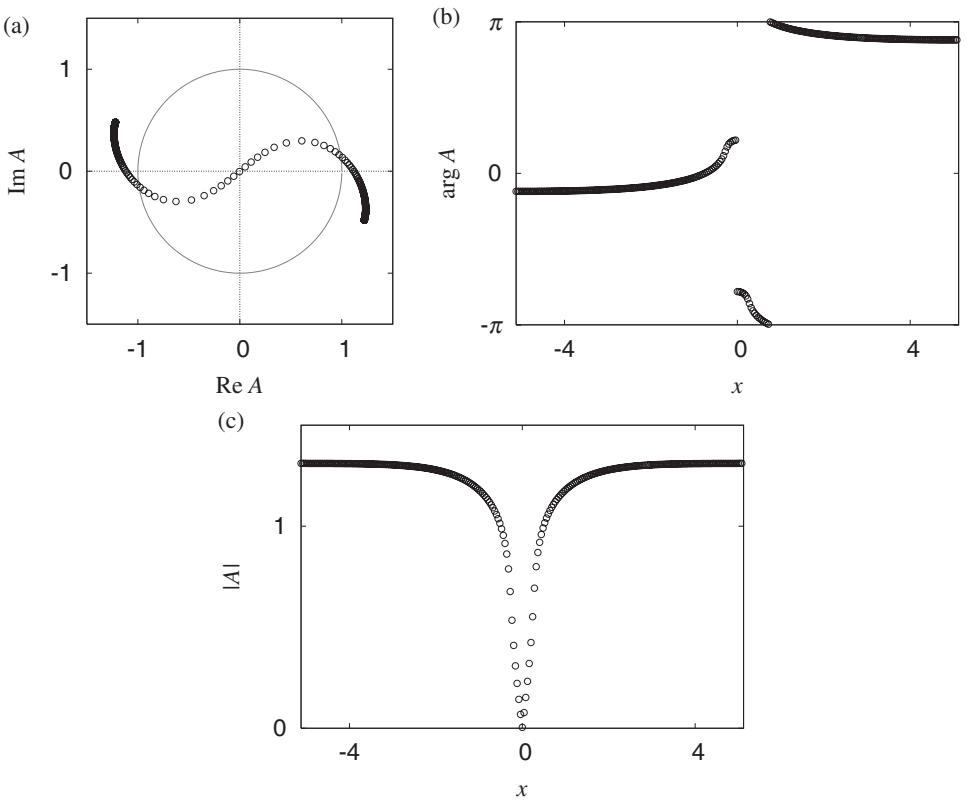

FIG. 1. Phase portrait (a), spatial phase profile (b), and spatial modulus profile (c) of the normal Ising wall exhibited by the forced nonlocally coupled complex Ginzburg-Landau equation (1) in the strong coupling case, $K=1.5$ and $\gamma=1.0$. The numerical data are represented by the open circles (only one in every eight oscillators is plotted). The limit-cycle orbit $|A|=1$ of the local oscillator is also displayed in (a).

ciently small and fixed separation $\Delta x=0.005$, i.e., $L=N\Delta x$, and the Neumann boundary condition (zero flux) was imposed. Our numerical results are unchanged if we further increase the number of grid points N or the system size L. The initial condition was such that $A\ (x<0,t=0)=1.0$ and $A\ (x\geqslant 0,t=0)=-1.0$. In what follows, we fix the parameter values as $c_0=1.0$, $c_1=-0.5$, and $c_2=1.0$. Note that we set the frequency mismatch at zero, i.e., $c_0-c_2=0$, for the sake of simplicity. Furthermore, we fix the ratio of the coupling strength to the force intensity as $K/\gamma=1.5$.

Figure 1 displays a phase portrait [Fig. 1(a)], a spatial profile of the phase [Fig. 1(b)], and a spatial profile of the modulus [Fig. 1(c)] for the strong coupling case, $K=1.5$ and $\gamma=1.0$, obtained by a direct numerical simulation of Eq. (1). The phase portrait is given by a set of grid points in the complex plane, each representing the state of a local oscillator at a given time. It is found that a normal Ising wall appears and all local oscillators are completely phase locked.

Figure 2 displays a phase portrait [Fig. 2(a)], a spatial profile of the phase [Fig. 2(b)], and a spatial profile of the modulus [Fig. 2(c)] for the weak coupling case, $K=0.06$ and $\gamma=0.04$. It is found that a chimera Ising wall appears, which consists of incoherent drifting oscillators near the center $(x=0)$ and coherent phase-locked oscillators in the peripheral regions. All the oscillators take almost the full amplitude $|A|=1$, so that the system has no phase singularity. At the same time, the spatial continuity of the pattern near the center $(x=0)$ is lost, so that a pair of local oscillators infinitely close to each other in this region are not always close in the state space.

We can estimate the critical coupling strength below which the oscillator at the center of the normal Ising wall starts to drift incoherently, leading to the chimera state. From the spatial symmetry of the normal Ising wall, the values of A and B vanish at the center, i.e., $A\ (x=0,t)=B\ (x=0,t)=0$. If we regard B as an external forcing [4], the linearized equation for the complex amplitude $A\ (x=0,t)$ at the center is given by

$$\partial_t A = (1+ic_0)A - K(1+ic_1)A + \gamma A^*. \tag{4}$$

A linear stability analysis of the stationary solution $A\ (x=0,t)=0$ gives the following eigenvalues:

$$\lambda_\pm = 1 - K \pm \sqrt{\gamma^2 - (c_0 - Kc_1)^2}. \tag{5}$$

Therefore, the necessary condition for the appearance of the chimera Ising wall, i.e., the condition for the oscillator at the center $(x=0)$ to drift, is expressed as $\lambda_+>0$. In fact, when $K<1$ is satisfied under our parameter conditions, the oscillator at the center $(x=0)$ starts to drift and a chimera Ising wall appears. Hereafter, we focus on the chimera Ising walls and consider the situation where the coupling strength is much smaller than 1, i.e., $K\ll 1$.

III. PHASE REDUCTION

In order to investigate the nature and the origin of the chimera Ising walls in further detail, we reduce Eq. (1) to a phase equation for the phase $\phi(x,t)$, which is much easier to analyze. When the coupling strength K and the forcing intensity γ are sufficiently small, the phase reduction method [21–23] is applicable, which is actually the case for our weak coupling case, $K=0.06$ and $\gamma=0.04$. The reduced equation takes the form

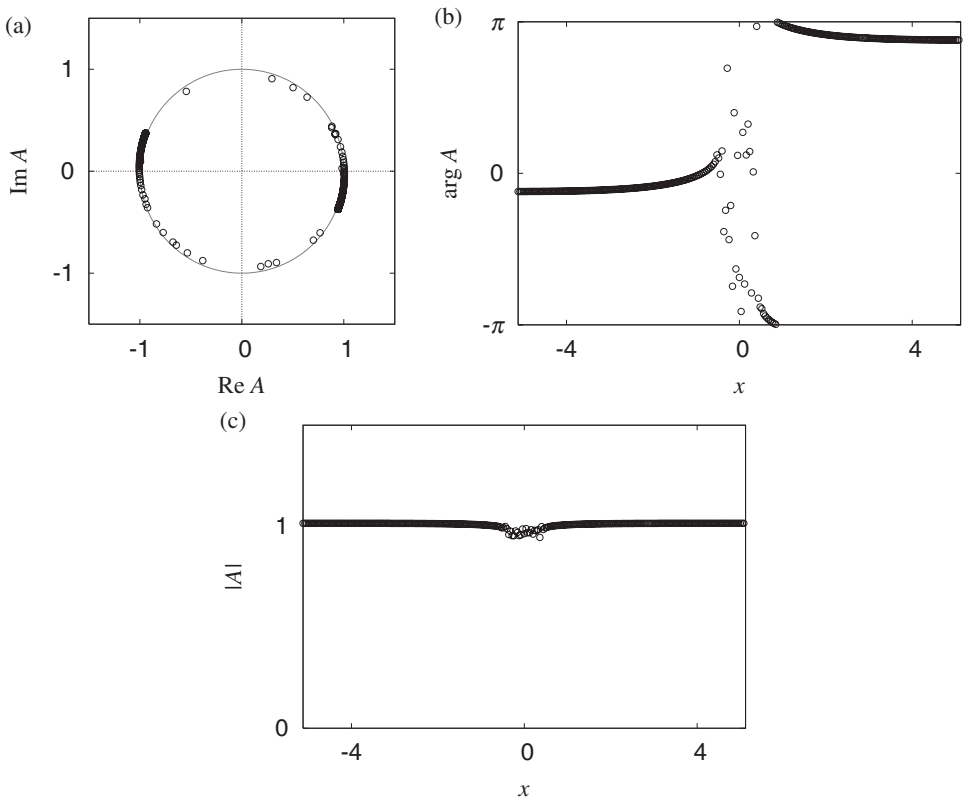

FIG. 2. Phase portrait (a), spatial phase profile (b), and spatial modulus profile (c) of the chimera Ising wall exhibited by the forced nonlocally coupled complex Ginzburg-Landau equation (1) in the weak coupling case, $K=0.06$ and $\gamma=0.04$. The numerical data are represented by the open circles (only one in every eight oscillators is plotted). The limit-cycle orbit $|A|=1$ of the local oscillator is also shown in (a).

$$\partial_t \phi = -K\sigma \int dx' G(x-x')[\sin(\phi-\phi'+\alpha)-\sin\alpha] - \gamma\tau\sin(2\phi+\beta), \tag{6}$$

where the condition $c_0-c_2=0$ was used. Here ϕ' is the abbreviation of $\phi(x',t)$. The new parameters are related to the original parameters through

$$\sigma\exp(i\alpha) = (1-ic_1)(1+ic_2), \tag{7}$$

$$\tau\exp(i\beta) = (1+ic_2), \tag{8}$$

where σ, τ, α, and β are real. When the time scale is changed so that the force intensity is normalized, $t\to t/\gamma\tau$, Eq. (6) can be rewritten as

$$\partial_t \phi = -K_\gamma \int dx' G(x-x')[\sin(\phi-\phi'+\alpha)-\sin\alpha] - \sin(2\phi+\beta), \tag{9}$$

where

$$K_\gamma = \frac{K\sigma}{\gamma\tau}. \tag{10}$$

Figure 3(a) displays a spatial profile of the phase ϕ of the local oscillators obtained by a numerical simulation of Eq. (9) using parameter conditions corresponding to Fig. 2. The phase pattern is very similar to that in Fig. 2(b). As in the previous case, only the local oscillators near the center ($x=0$) are drifting incoherently, and all other oscillators are phase locked.

Now let us introduce a space-dependent complex order parameter with modulus $R(x)$ and phase $\Phi(x)$ through

$$R(x)\exp[i\Phi(x)] = \int dx' G(x-x')\exp[i\phi(x',t)]. \tag{11}$$

We assume the order parameter to be time independent, which will be confirmed below. In terms of this order parameter, Eq. (9) may be expressed in the form of a single-oscillator equation

$$\partial_t \phi = -K_\gamma[R\sin(\phi-\Phi+\alpha)-\sin\alpha] - \sin(2\phi+\beta), \tag{12}$$

or, if we further introduce a space-dependent effective force function $H_x(\phi)$ through

$$H_x(\phi) = K_\gamma[R\sin(\phi-\Phi+\alpha)-\sin\alpha] + \sin(2\phi+\beta), \tag{13}$$

Eq. (9) can be expressed as

$$\partial_t \phi = -H_x(\phi). \tag{14}$$

Our effective force function is composed of the internal force (the first harmonic term) and the external force (the second harmonic term), which is similar to the order function introduced by Daido [24–26].

The spatial profiles of $R(x)$ and $\Phi(x)$ obtained by the numerical simulation of Eq. (9) are displayed in Figs. 3(b) and 3(c), respectively. We can see that the order-parameter modulus has a vanishing value at the center, and both the modulus and the phase of the order parameter are time independent. The distribution of the mean frequency $\bar{\omega}(x)$ of the local

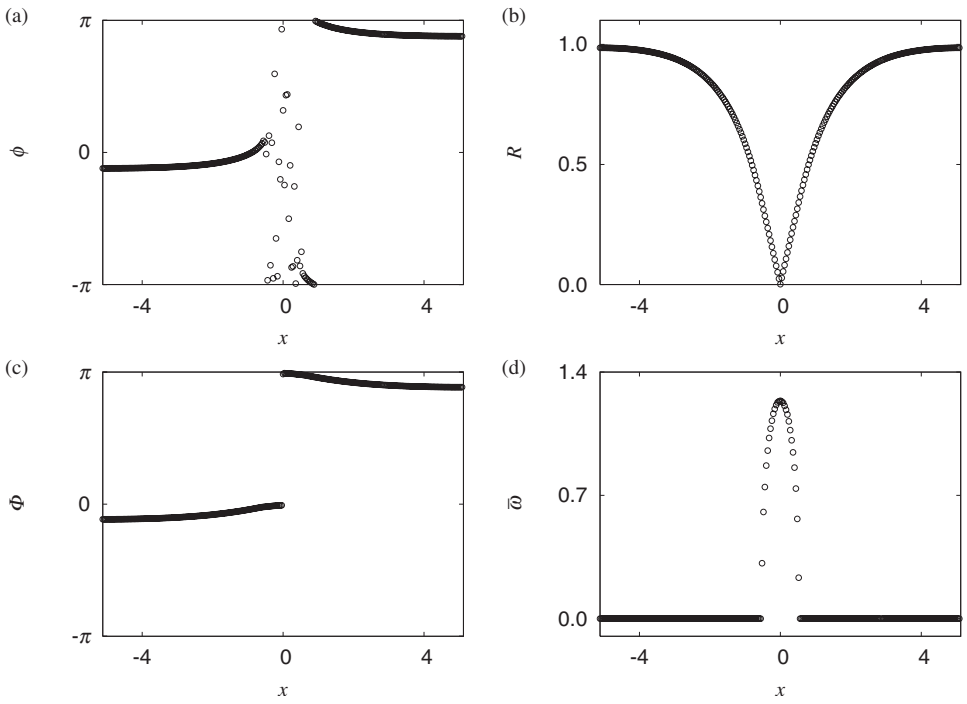

FIG. 3. Spatial profiles of the local oscillator phase ϕ (a), the order-parameter modulus R (b), the order-parameter phase Φ (c), and the mean frequency $\bar{\omega}$ of the local oscillators (d), obtained by a numerical simulation of the phase equation (9). The numerical data are represented by open circles (only one in every eight oscillators is plotted).

oscillators, which is defined by the long-time average of $\partial_t \phi$, is also displayed in Fig. 3(d). In the phase-locked domain, the oscillation frequencies are identically zero, while in the drifting domain they are distributed.

The dependence of the effective force function $H_x(\phi)$ on x and ϕ is displayed in Fig. 4. It is found that $H_x(\phi)$ crosses the zero plane only twice in every 2π interval of ϕ at each x in the peripheral regions, which will make our analysis simple. We should also note that $H_x(\phi)$ is always below zero near the center ($x=0$), namely, $H_x(\phi)$ never crosses the zero plane in this region.

In the next section, we develop a self-consistent theory for determining the spatial profiles of the quantities displayed in Fig. 3.

IV. SELF-CONSISTENT THEORY

We now develop a self-consistent theory that can reproduce our simulation results by generalizing the earlier theories [1–4,21–26]. There are two possible cases regarding the solution of Eq. (14). Let $H_{\min}(x)$ and $H_{\max}(x)$ denote the minimum and the maximum of $H_x(\phi)$ in every 2π interval of ϕ at each x, respectively. Then the two cases are expressed by

$$H_{\min}(x) < 0 < H_{\max}(x) \quad \text{(case I)} \tag{15}$$

and

$$H_{\min}(x) > 0 \quad \text{or} \quad 0 > H_{\max}(x) \quad \text{(case II)}. \tag{16}$$

Correspondingly, the oscillators are divided into two groups. In case I, which corresponds to the group of phase-locked oscillators in the peripheral regions, Eq. (14) admits only one pair of stable and unstable fixed points. We denote the stable fixed point formally as

$$\phi_0(x) = H_x^{-1}(0), \tag{17}$$

where H_x^{-1} is the inverse function of H_x. The average frequency $\bar{\omega}(x)$ of the oscillators in this group is identically zero,

$$\bar{\omega}(x) = 0. \tag{18}$$

Case II corresponds to the group of drifting oscillators, for which Eq. (14) admits a drifting solution. The average frequency $\bar{\omega}(x)$ is formally expressed as

$$\bar{\omega}(x) = 2\pi \left(\int_0^{2\pi} \frac{d\phi}{-H_x(\phi)} \right)^{-1}, \tag{19}$$

which depends on x. The contribution to the order parameter from the drifting oscillators can be computed by the standard method [1,21]. That is, we use the invariant measure, i.e., the probability density $p_x(\phi)$ associated with the drift motion. Noting that the probability density for the phase at x to take on value ϕ must be inversely proportional to the drift veloc-

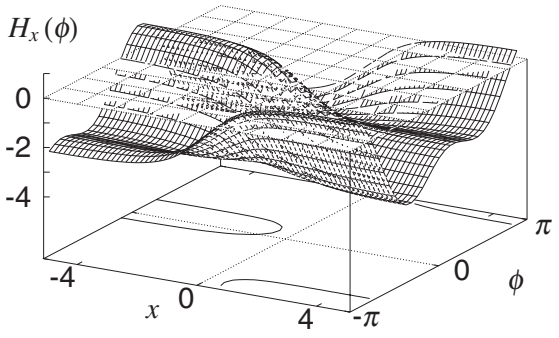

FIG. 4. Dependence of the effective force function $H_x(\phi)$ on x and ϕ. The contour lines corresponding to $H_x(\phi)=0$ are also displayed in the base plane. Note the gap near the center ($x=0$), where $H_x(\phi)$ does not cross the zero plane.

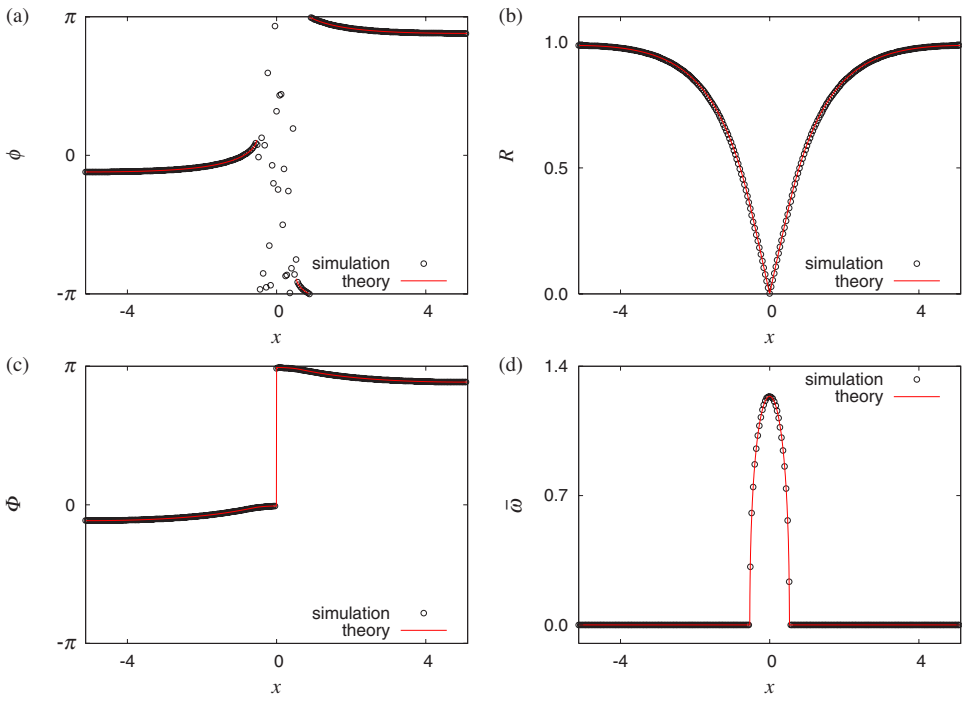

FIG. 5. (Color online) Comparison between the theory and the simulation results: Spatial profiles of the local oscillator phase ϕ (a), the order-parameter modulus R (b), the order-parameter phase Φ (c), and the mean frequency $\bar{\omega}$ of the local oscillators (d). The open circles and the solid lines are the simulation data and the theoretical curves, respectively.

ity given by the right-hand side of Eq. (14), we obtain

$$p_x(\phi) = C_x[-H_x(\phi)]^{-1}, \tag{20}$$

where C_x is the normalization constant given by

$$C_x = \left(\int_0^{2\pi} \frac{d\phi}{-H_x(\phi)} \right)^{-1}. \tag{21}$$

Putting together the two types of contributions to the order parameter, we finally obtain a functional self-consistency equation in the form

$$R(x)\exp[i\Phi(x)] = \int dx' G(x-x')h(x'), \tag{22}$$

where

$$h(x) = \begin{cases} e^{i\phi_0(x)} & \text{(case I)}, \\ \displaystyle\int_0^{2\pi} p_x(\phi)e^{i\phi}d\phi & \text{(case II)}. \end{cases} \tag{23}$$

We can determine the quantities shown in Fig. 3 from this functional self-consistency equation. The solution can be obtained numerically by an iteration procedure, which is compared with the results of the numerical simulation in Fig. 5. The agreement between the theory and the numerical simulation is excellent for all quantities.

We finally make a brief comment. The order-parameter phase does not drift in our chimera Ising walls, which makes our analysis easy because we do not need to calculate the collective frequency. In the two earlier examples of the chimera states, we had to work with a nonlinear eigenvalue problem, or determine the various quantities together with the collective frequency (i.e., the eigenvalue) [1,2].

V. CONCLUDING REMARKS

We present a type of chimera state associated with the Ising walls in the one-dimensional forced nonlocally coupled complex Ginzburg-Landau equation. We focused on the weak coupling case, where the phase reduction method is applicable, and reduced the original model to the phase model. Generalizing the previous theories, we derived a functional self-consistency equation to be satisfied by the order parameter. Its solution successfully reproduced our simulation results carried out on this phase model.

The chimera state studied in Refs. [1,3] seems rather special because the boundary effects are crucial [4]. In contrast, the chimera Ising walls stably exist regardless of the boundary effects, and they survive even in spatially infinitely extended systems, like the chimera spiral waves that persist in two-dimensional spatially extended systems [2,4]. Our preliminary analysis suggests that a chimera hole solution does not seem to exist in a one-dimensional nonlocally coupled (cubic) complex Ginzburg-Landau equation without parametric forcing. Therefore, our chimera Ising wall may be the simplest example of chimera states which is still relevant to real-world phenomena.

ACKNOWLEDGMENTS

The author is grateful to Y. Kuramoto, D. Battogtokh, H. Nakao, and S. Shima for valuable discussions.

[1] Y. Kuramoto and D. Battogtokh, Nonlinear Phenom. Complex Syst. (Dordrecht, Neth.) **5**, 380 (2002).
[2] S. I. Shima and Y. Kuramoto, Phys. Rev. E **69**, 036213 (2004).
[3] D. M. Abrams and S. H. Strogatz, Phys. Rev. Lett. **93**, 174102 (2004); Int. J. Bifurcation Chaos Appl. Sci. Eng. **16**, 21 (2006).
[4] Y. Kuramoto *et al.*, Prog. Theor. Phys. Suppl. **161**, 127 (2006).
[5] H. Sakaguchi, Phys. Rev. E **73**, 031907 (2006).
[6] Y. Kuramoto, Prog. Theor. Phys. **94**, 321 (1995); Int. J. Bifurcation Chaos Appl. Sci. Eng. **7**, 789 (1997).
[7] Y. Kuramoto and H. Nakao, Physica D **103**, 294 (1997); D. Battogtokh and Y. Kuramoto, Phys. Rev. E **61**, 3227 (2000).
[8] Y. Kuramoto, D. Battogtokh, and H. Nakao, Phys. Rev. Lett. **81**, 3543 (1998).
[9] H. Nakao, Chaos **9**, 902 (1999).
[10] D. Tanaka and Y. Kuramoto, Phys. Rev. E **68**, 026219 (2003).
[11] S. C. Manrubia, A. S. Mikhailov, and D. H. Zanette, *Emergence of Dynamical Order* (World Scientific, Singapore, 2004).
[12] V. Casagrande and A. S. Mikhailov, Physica D **205**, 154 (2005).
[13] P. Coullet, J. Lega, B. Houchmanzadeh, and J. Lajzerowicz, Phys. Rev. Lett. **65**, 1352 (1990); P. Coullet and K. Emilsson, Physica D **61**, 119 (1992).
[14] T. Mizuguchi and S. Sasa, Prog. Theor. Phys. **89**, 599 (1993).
[15] T. Ohta, J. Kiyose, and M. Mimura, J. Phys. Soc. Jpn. **66**, 1551 (1997).
[16] D. Battogtokh and D. Browne, Phys. Lett. A **266**, 359 (2000).
[17] I. S. Aranson and L. Kramer, Rev. Mod. Phys. **74**, 99 (2002).
[18] T. Teramoto, K.-I. Ueda, and Y. Nishiura, Phys. Rev. E **69**, 056224 (2004); Prog. Theor. Phys. Suppl. **161**, 364 (2006).
[19] M. U. Kobayashi and T. Mizuguchi, Phys. Rev. E **73**, 016212 (2006); Prog. Theor. Phys. Suppl. **161**, 228 (2006).
[20] D. Battogtokh (private communication); in Proceedings of the International Symposium on Oscillation, Chaos and Network Dynamics in Nonlinear Science (OCNN2004), Kyoto, 2004 (unpublished), p. 24.
[21] Y. Kuramoto, *Chemical Oscillations, Waves, and Turbulence* (Springer, New York, 1984; Dover, New York, 2003).
[22] A. Pikovsky, M. Rosenblum, and J. Kurths, *Synchronization* (Cambridge University Press, Cambridge, U.K., 2001).
[23] A. T. Winfree, *The Geometry of Biological Time*, 2nd ed. (Springer, New York, 2001).
[24] H. Daido, Prog. Theor. Phys. **88**, 1213 (1992); **89**, 929 (1993); Phys. Rev. Lett. **73**, 760 (1994); Physica D **91**, 24 (1996); Int. J. Bifurcation Chaos Appl. Sci. Eng. **7**, 807 (1997).
[25] S. H. Strogatz, Physica D **143**, 1 (2000).
[26] J. A. Acebrón *et al.*, Rev. Mod. Phys. **77**, 137 (2005).